

## REMOVAL OF ARSENIC USING MESOPOROUS SILICATE MEDIA IMPREGNATED METAL OXIDES NANO-PARTICLES

Min Jang<sup>1</sup>, Eun Woo Shin<sup>2</sup>, and Jae Kwang Park<sup>1</sup>

<sup>1</sup>Department of Civil and Environmental Engineering, University of Wisconsin-Madison,  
1415 Engineering Drive, Madison, WI 53706 USA

<sup>2</sup>Forest Products Laboratory, USDA, One Gifford Pinchot Drive,  
Madison, WI 53705 USA

### ABSTRACT

The highly ordered mesoporous silica SBA-15 was successfully synthesized and incorporated with iron, aluminum, and zinc oxides by use of an incipient wetness impregnation technique. Aluminum 10% impregnation was safely incorporated by an incipient wetness impregnation technique for SBA-15, which had 638.75 m<sup>2</sup>/g of BET surface area and 48 Å of pore diameter, without producing clogging of pore structures. The adsorption capacities of these materials were evaluated with adsorption isotherm and kinetic studies under different batch conditions. Aluminum was the best incorporation metal compound and impregnation of aluminum 10% for SBA-15 had greater than 2 times higher arsenate adsorption capacity and 15 times higher rate than activated alumina under the condition of 0.133 mmol/L arsenate initial concentration and 0.333 g/L of solids concentration. Al<sub>10</sub>SBA-15 showed about 2.2 ~ 2.4 times higher arsenate adsorption capacities than activated alumina in a broad range of arsenate initial concentrations, in which the *Freundlich* isotherm model was fitted very well. The rate-controlling step of arsenate adsorption for all adsorbents appeared to be explained by both the exchange reaction and diffusion reaction. These results showed great advantages of Al<sub>10</sub>SBA-15 for POE/POU application due to its rapid and high adsorption capacity.

### KEYWORDS

**Arsenate, mesoporous, SBA-15, and nano-particles**

## INTRODUCTION

Throughout the world, arsenic is creating potentially serious environmental problems for human and other living organisms. Most reported arsenic problems in water supply systems have been found in groundwater, usually the drinking water source in rural areas, which have been mainly caused by human activities such as mining wastes, petroleum refining, sewage sludges, agricultural chemicals, ceramic manufacturing industries and coal fly ash (Viraraghavan *et al.*, 1999). Natural causes include mineral weathering and dissolution caused by the changes of geo-chemical environments to reductive conditions (Namasivayam and Senthilkumar, 1998; Chris *et al.*, 2000).

By reducing the regulation limit of arsenic contamination from 50 to 10 ppb, as announced by the Bush administration on October 31, 2001, small public water systems will face heavy financial burdens for complying with stringent limits on arsenic (Woods, 2001).

Therefore, a highly effective, reliable, and economical technique is needed to meet the new arsenic maximum contaminant level. Compared to other techniques, adsorption usually does not need a large area or additional chemicals for treatment, and does not generate sludge. It is also very easy to set up the POE/POU (Point of Use/Point of Entry) process. For the POE/POU system, activated alumina has been one of the best available adsorbents and has been extensively studied because it is very effective and selective for arsenic adsorption removal (Gilles, 2000). However, the highly alkaline feeding solution should be controlled with acidic solution to have pH 5.5~6.0 to achieve optimum arsenic adsorption capacity of activated alumina (Chwirka *et al.*, 2000). In addition, when activated alumina is regenerated, its adsorption capacity will be reduced by 20 ~ 50%. Furthermore, due to the slower adsorption reaction, activated alumina should have relatively longer empty bed contact time than ion exchange resins (Johnston and Heijnen, 2001).

The M41 S family of mesoporous silicate molecular sieves, developed by Mobil scientists in 1992, has opened up new possibilities in the fields of catalysis, sensors, and adsorbents (Kresge *et al.*, 1992). These materials are synthesized with a self-assembled molecular array of surfactant molecules as a structure-directing template, which results in very sharp and ordered pore distributions of inorganic materials. These materials can be classified with different pore structures as following MCM-41 (two dimensional hexagonal mesopore structure), MCM-48 (three dimensional cubic mesopore structure), and MCM-50 (lamellar mesopore structure).

The newly developed mesoporous silica molecular sieves, so called SBA-15, were successfully synthesized using amphiphilic triblock copolymers as a structure-directing template agent under hydrothermal conditions. It has uniform two dimensional hexagonal (space group  $p6mm$ ) mesopore channels that can be tailored by changing the synthesis conditions (Zhao *et al.*, 1998). Compared with the M41 S types which were developed by Mobil scientists, the mesoporous silica SBA-15 molecular sieve had larger pore sizes of about 50~100 Å, without pore expanding chemicals, so that it has a good

possibility to incorporate a large portion of metal precursor without blocking effects. In addition, water or ethanol extraction can be applied to recover the pore-forming template for reuse in SBA-15 synthesis due to the weak interaction between two dimensional hexagonal silica and triblock copolymer mesophases (Kruk *et al.*, 2000).

Through several incorporation techniques, the organic or inorganic materials can be functionalized onto the monolayer of highly ordered nano-structured materials having a huge amount of surface area in a very small volume to make highly active sites for the applications of adsorption, catalysis, or sensor. Up to now, due to their advanced characteristics, the incorporation of functioning materials for mesoporous materials have been spotlighted in terms of synthesis, mechanism, and applications (Kruk *et al.*, 2000; Margolese *et al.*, 2000; Zhao *et al.*, 2000; Newalkar *et al.*, 2001).

The objectives of this study were to develop novel adsorbents through synthesizing highly ordered mesoporous silica SBA-15 and incorporating nano-particles of metal oxides by use of an incipient-wetness impregnation technique and to evaluate the adsorption capacities of arsenic species through adsorption kinetics and isotherm studies with different conditions for the metal oxides incorporated SBA-15.

## METHODOLOGY

### Synthesis of metal oxide impregnated SBA-15

SBA-15 was synthesized using triblock copolymer (Pluronic P123,  $\text{EO}_{20}\text{PO}_{70}\text{EO}_{20}$ ) (Aldrich) as a structuredirecting reagent and tetraethyl orthosilicate (Aldrich) as a silica precursor. A 4 gram triblock copolymer was dissolved in deionized water for 30 min. Then, a 2 M hydrochloric acid solution was added. The mixed solution was stirred for 30 minutes. Next, tetraethyl orthosilicate (TEOS) was added to the mixture and heated at 45°C for 20 hrs. The mixture was transferred into a Teflon bottle and heated at 80°C for 24 hrs without stirring. After that, the solid product was filtered with 0.45  $\mu\text{m}$  filter paper and dried at room temperature with vacuum before calcination. The mole fraction of each component for as-synthesized SBA-15 was 1 mol TEOS:5.854 mol HCl:162.681 mol  $\text{H}_2\text{O}$ :0.0168 mol triblock copolymer. The calcination was performed in an oven at 550°C for 6 hrs in air to remove the triblock copolymer organic component. The calcined SBA-15 was preserved at room temperature under vacuum.  $(\text{NO}_3)_2 \cdot 9\text{H}_2\text{O}$ ,  $\text{Fe}(\text{NO}_3)_3 \cdot 9\text{H}_2\text{O}$ , and  $\text{Zn}(\text{NO}_3)_2 \cdot 6\text{H}_2\text{O}$  were selected as aluminum, iron, and zinc precursors to incorporate into SBA-15 through use of the incipient wetness impregnation technique. Each metal precursor was dissolved in the deionized water at the given concentrations. The metal precursor solution was evenly distributed by a small volume with a 200  $\mu\text{L}$  micropipette for SBA-15, which was placed in the mortar. Then, the mixture was homogeneously mixed with a pestle for 5 min. This procedure was repeated until the ratio of metal precursor solution volume (mL) and SBA-15 mass (grams) was two. The mixture was dried in the hood at room temperature for 1 day. The solids were then calcined in an oven with the programmed temperature of the range from room temperature to 400°C with the speed of 0.5°C per minute. After calcination, the solids were kept on the vacuum chamber.

After synthesizing Al<sub>10</sub>SBA-15, the conductivity tests were performed to confirm the oxidation of the aluminum precursor. Exactly 0.02 g of Al<sub>10</sub>SBA-15 was washed with 5 mL of deionized water and filtered out with a 0.45 μm filter. The conductivity of the filtrate was analyzed with a conductance meter (YSI model 32). The conductivity was 10 ohms, which is the same as that of deionized water, indicating no leaching of aluminum precursor.

### Characterization of media

X-ray diffraction patterns were obtained using a Stoe High Resolution X-Ray Diffractometer equipped with CuKα radiation (40 kV, 25 mA) with a 0.05° step size and 5 second step time over the range 0.8° < 2θ < 6.0°. N<sub>2</sub> gas adsorption isotherms were performed at 77 K using a Micromeritics ASAP 2010 analyzer. SBA-15 was dehydrated at 250°C for 1 day before taking the isotherm data. The BET specific surface area was calculated by the linear part of the BET equation. The pore size distributions of media were obtained using Barrett, Joyner and Halenda (BJH) analysis of the desorption branch of the hysteresis loop of the nitrogen adsorption isotherm. The pore diameter (D<sub>BJH</sub>), mesopore surface area (A<sub>BJH</sub>), and volume (V<sub>BJH</sub>) were calculated by the pore size distribution curves. The pore diameter (D<sub>BJH</sub>) was calculated with  $4 V_{BJH}/A_{BJH}$ .

### Arsenate adsorption isotherm tests

Sodium arsenate (Na<sub>2</sub>HAsO<sub>4</sub> · 7H<sub>2</sub>O (Sigma) was used as the arsenate source without any modification. A stock solution of arsenate was prepared with 133 mmol As/L in the deionized water prepared with the Millipore System. NaNO<sub>3</sub> (0.01 M) solution prepared with deionized water was poured into a polyethylene bottle of given volume. Then, a small volume of arsenic stock solution was added to achieve the given arsenic concentration and the pH of suspension was adjusted with a pH automatic titrator. All samples were set into a rotary shaker and shaken at 250 rpm. The shaking temperature was 25 ± 0.5°C. After 8 hrs of shaking, the pH of samples was readjusted with the pH automatic titrator, using small volumes of acid and base stock solution. All samples then were reset in the rotary shaker to achieve equilibrium state. After 24 hrs of shaking, 5 mL of the suspension was withdrawn and filtered immediately with a 0.45 μm pre-rinsed Uniflo filter unit.

All data of the arsenic adsorption isotherm were fitted with *Freundlich* and *Langmuir* isotherm models.

### Adsorption kinetics

The preparation of arsenate stock solution was the same as the adsorption isotherm tests. An aliquot of 300 mL of deionized water was prepared with a given concentration of NaNO<sub>3</sub> and poured into a reaction bottle for each kinetic study. After injecting a small volume of arsenic stock solution to make the planned arsenic concentration, the

suspension was stirred with 500  $\mu\text{m}$  of stirring velocity on the magnetic stirrer. The pH of the solution was adjusted with an automatic titrator and the temperature was maintained at  $25 \pm 0.5^\circ\text{C}$  for one hour before the adsorbent was injected at a predetermined mass. In order to maintain a constant pH during kinetic studies, the automatic titrator was set up in the reactor, connected with a pH electrode and small tubes coming from two pumps which could titrate with small volume of acid ( $\text{HNO}_3$ , 0.1 M) and base ( $\text{NaOH}$ , 0.1 M) stock solution. One of the two pumps for acid and base stock solution was operated when the pH drifted  $\pm 0.02$  pH units from the initial pH. An aliquot of 3 mL of suspensions was withdrawn at 2~60 minute periods and filtered through a 0.45  $\mu\text{m}$  Uniflo filter unit for arsenic analysis. Activated alumina (Aldrich) was selected to compare the adsorption isotherm and kinetic data with aluminum impregnated SBA-15.

All of the kinetic data was fitted with different kinetic models such as pseudo first, pseudo second, power function, simple Elovich and parabolic diffusion, which are described in Table 1.

**Table 1 -Equations for Fitting Different Kinetic Models**

Kinetic Models	Linear plots	Equations
Pseudo-first order	$\ln(q_{\text{eq}} - q_t)$ vs. $t$	$\ln(q_{\text{eq}} - q_t) = \ln(q_{\text{eq}}) - k_1 t$
Pseudo-second order	$t/q_{\text{eq}}$ vs. $t$	$\frac{t}{q_t} = \frac{1}{v_0} + \frac{1}{q_{\text{eq}}} t$
Power function	$\ln(q_t)$ vs. $\ln(t)$	$\ln(q_t) = \ln a + b \ln(t)$
Parabolic diffusion	$q_t/q_{\text{eq}}/t$ vs. $t^{-0.5}$	$\frac{q_t}{q_{\text{eq}} t} = k_{\text{diff}} t^{-0.5} + a$
Simplified Elovich	$q_t$ vs. $\ln(t)$	$q_t = a \ln(t) + b$

$q_{\text{eq}}$  = adsorbed arsenic at equilibrium,  $t$  = adsorption reaction time,  $q_t$  = adsorbed arsenic at time  $t$ ,  $k_1$  ( $\text{min}^{-1}$ ) = pseudo first order adsorption rate constant,  $v_0$  (initial sorption rate,  $\text{mmol g}^{-1} \text{min}^{-1}$ ) =  $k_2 q_{\text{eq}}$ ,  $k_2$  ( $\text{g mmol}^{-1} \text{min}^{-1}$ ) = pseudo second order adsorption rate constant,  $k_{\text{diff}}$  ( $\text{min}^{-0.5}$ ) = overall diffusion adsorption rate constant, and,  $a$  and  $b$  are constants.

### Arsenic analysis

Aluminum and high concentrations of arsenate were analyzed with an Inductively Coupled Plasma Atomic Emission Spectrometer (ULTIMA, John Yvon Inc.) and a Varian AA-975 Atomic Absorption Spectrophotometer and GTA-95 Graphite Tube Atomizer with programmable sample dispenser were used for samples having low arsenate concentrations. As a matrix modifier, 20 mg/L nickel solution was used.

## RESULTS AND DISCUSSION

### X-ray diffraction

As Figure 1 shows, calcined SBA-15 displayed a well-resolved pattern at very low angles with a sharp peak at  $0.95^\circ$  and two weak peaks at  $1.65^\circ$  and  $1.90^\circ$ . This x-ray diffraction pattern was similar with reported SBA-15 (Zhao *et al.*, 1998). The XRD peaks can be indexed to a hexagonal lattice with a  $d_{100}$  spacing of  $92.91 \text{ \AA}$ , corresponding to a large unit cell parameter  $a_0$  of  $107.3 \text{ \AA}$ , obtained by the following equation:  $a_0 = 2 \times d_{100} / \sqrt{3}$ . The intensities of peaks were decreased after incorporating 10% metals into SBA-15. The decrease in peaks intensities were in the following orders: Fe > Al > Zn, which demonstrate the same trends for heterogeneity of pore structure. However, every 10% metal was safely incorporated without creating significant clogging of the pore structures. Especially, all peak positions of  $\text{Al}_{10}\text{SBA-15}$  were shifted to have smaller  $d_{100}$  and  $a_0$  values which are  $88.27 \text{ \AA}$ , and  $101.9 \text{ \AA}$ , respectively. This result showed that 10% of aluminum incorporation caused the reduction of pore structures. However, the peaks were not shifted in the case of zinc and iron impregnations.

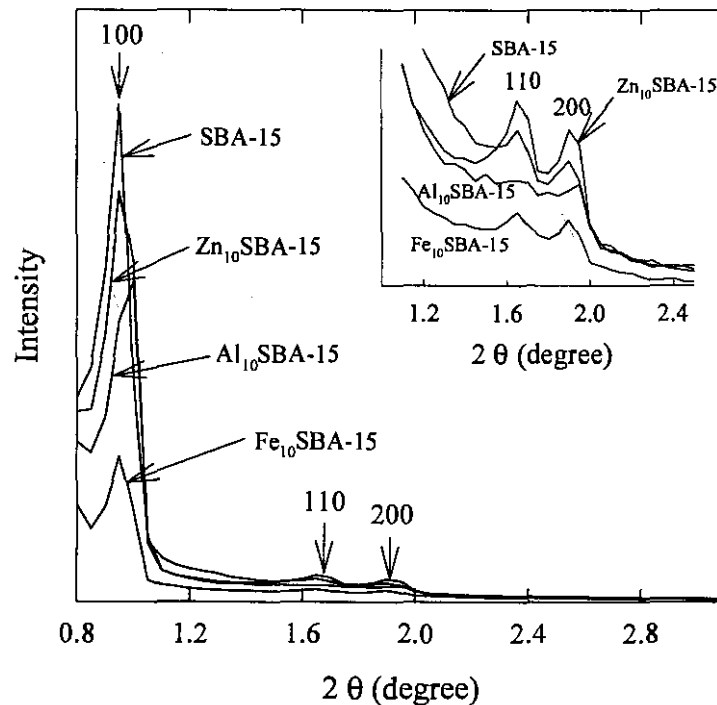
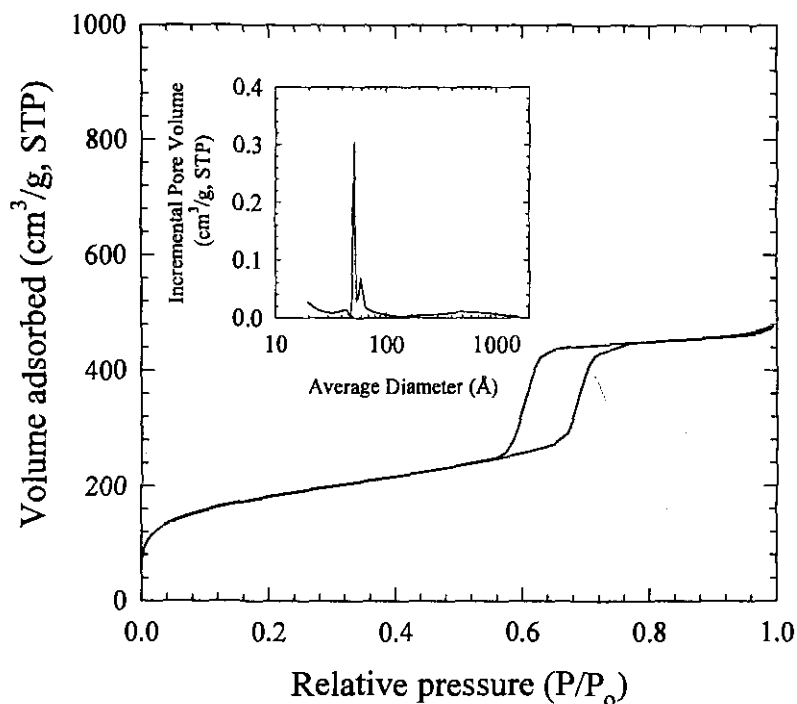


Figure 1 - X-ray diffraction pattern for calcined SBA-15, Al, Fe, and Zn 10% impregnated SBA-15

### Nitrogen adsorption isotherm

$N_2$  adsorption-desorption isotherm results are shown in Figure 2. The calcined SBA-15 has a typical type IV adsorption isotherm following IUPAC classification and shows a H1 hysteresis loop which is representative for mesoporous media (Sing *et al.*, 1985). At relative pressure ( $P/P_0$ ) of about 0.68, sharp increases of adsorbed volume were started, showing capillary condensation of nitrogen within uniform mesopore structures.

Parameters of pore structure for SBA-15 were calculated from the desorption branch of nitrogen adsorption isotherms using the BJH formula.  $A_{BET}$ ,  $A_{BJH}$ ,  $V_{BJH}$ , and  $D_{BJH}$  values for calcined SBA-15 were  $638.75 \text{ m}^2/\text{g}$ ,  $644.96 \text{ m}^2/\text{g}$ ,  $0.776 \text{ cm}^3/\text{g}$ , and  $48.15 \text{ \AA}$ , respectively. The calcined SBA-15 showed a very sharp pore size distribution obtained by incremental pore volume according to the average pore diameter.



**Figure 2 - Adsorption-desorption isotherms of nitrogen at 77 K of calcined SBA-15 and pore size distribution obtained by incremental pore volume according to average pore diameter.**

### Arsenic adsorption isotherm

Figure 3 shows the arsenic adsorption isotherm results for all adsorbents at different arsenate initial concentrations. Arsenate was adsorbed on  $Fe_{10}$ SBA-15 and  $Al_{10}$ SBA-15 in greater amounts than activated alumina at higher arsenate concentrations. However,  $Zn_{10}$ SBA-15 did not have a good arsenate adsorption capacity. Compared with activated

alumina, which is mainly used for arsenic adsorption removal, aluminum 10% incorporated SBA-15 had a maximum adsorption capacity ( $Q_{\max}$ ) of 2.36 fold greater (Table 2). At the arsenate initial concentration of 1.33 mmol/L, the observed arsenate adsorption densities for activated alumina,  $Al_{10}$ SBA-15,  $Fe_{10}$ SBA-15, and  $Zn_{10}$ SBA-15 were 0.0067 mmol<sub>As</sub>/mmol<sub>Al</sub>, 0.073 mmol<sub>As</sub>/mmol<sub>Al</sub>, 0.103 mmol<sub>As</sub>/mmol<sub>Fe</sub>, and 0.012 mmol<sub>As</sub>/mmol<sub>Zn</sub> respectively. Therefore, based on the mole fraction of arsenate and each metal,  $Al_{10}$ SBA-15 and  $Fe_{10}$ SBA-15 had arsenate adsorption densities of 10.9 and 15.4 times higher than that of activated alumina. Therefore, dispersion of metal oxides onto the highly ordered nano-structured silica oxide can provide a good possibility of higher adsorption capacity due to the increase in active sites if clogging effects of metal oxides are not significant for SBA-15.

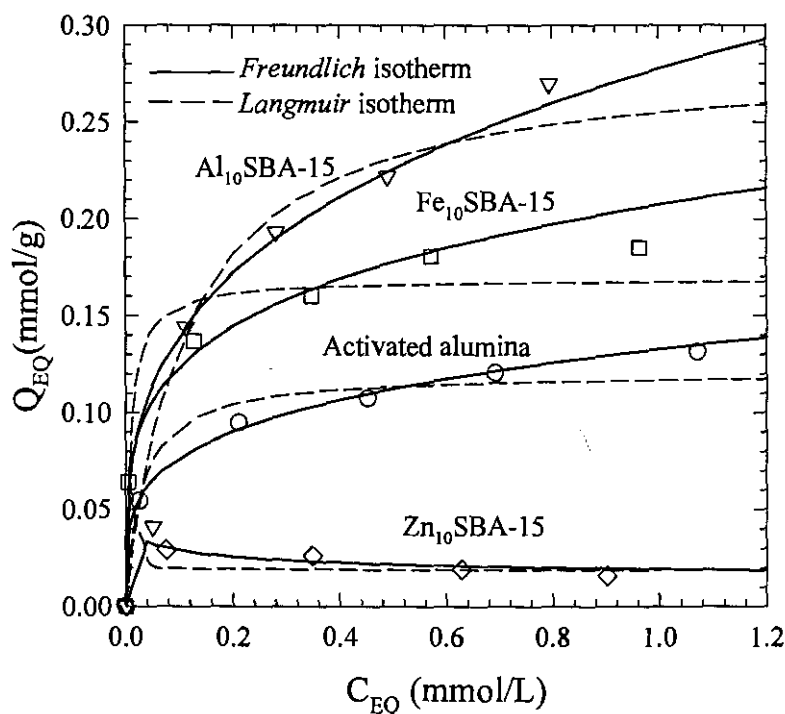


**Figure 3 - Arsenate adsorption isotherm (pH = 6.55, shaker temperature =  $25 \pm 0.5^\circ\text{C}$ , the ionic strength made by  $\text{NaNO}_3$  = 0.01 M). The solution volume and mass of each adsorbent were 50 mL and 0.1 g, respectively. After 24 hrs of shaking, 5 mL of the suspension was withdrawn and filtered immediately with 0.45  $\mu\text{m}$  pre-rinsed Uniflo filter unit. The filtrate was analyzed for arsenate concentration of solution with ICP-AES.**

After the equilibrium adsorption data were fitted with two different isotherm models; *Langmuir* and *Freundlich*, the fitting parameters and determination coefficient  $R^2$  values are summarized in Table 2. All isotherm data fit very well with the *Freundlich* isotherm model with almost  $>0.99$  of  $R^2$  values except the data of  $Zn_{10}$ SBA-15. The other metal compounds such as iron, aluminum, and zinc ions for aliquot were not detected by ICP-

AES. Therefore, it was confirmed that all of the metal precursors were completely oxidized to metal oxide under the calcination conditions used in this study.

**Table 2 - Determination Coefficients ( $R^2$ ) and Parameters for the Fit of Arsenate Adsorption Isotherm Data to Both *Freundlich* and *Langmuir* Isotherms**

Adsorption isotherms and parameters		Activated alumina	Al <sub>10</sub> SBA-15	Fe <sub>10</sub> SBA-15	Zn <sub>10</sub> SBA-15
<i>Langmuir</i>	b	32.824	8.935	108.119	-32.881
	Q <sub>max</sub> (mmol/g)	0.120	0.283	0.169	0.018
	R <sup>2</sup>	0.971	0.966	0.980	0.527
<i>Freundlich</i>	K	0.133	0.277	0.208	0.019
	n	0.239	0.298	0.225	-0.170
	R <sup>2</sup>	0.995	0.996	0.995	0.741

b, Q<sub>max</sub>, K, and n are fitting parameters for both adsorption isotherms

$$\text{Langmuir } (q_{eq} = \frac{bQ_{max}C_{eq}}{1 + bC_{eq}}) \text{ and Freundlich } (q_{eq} = KC_{eq}^{1/n}).$$

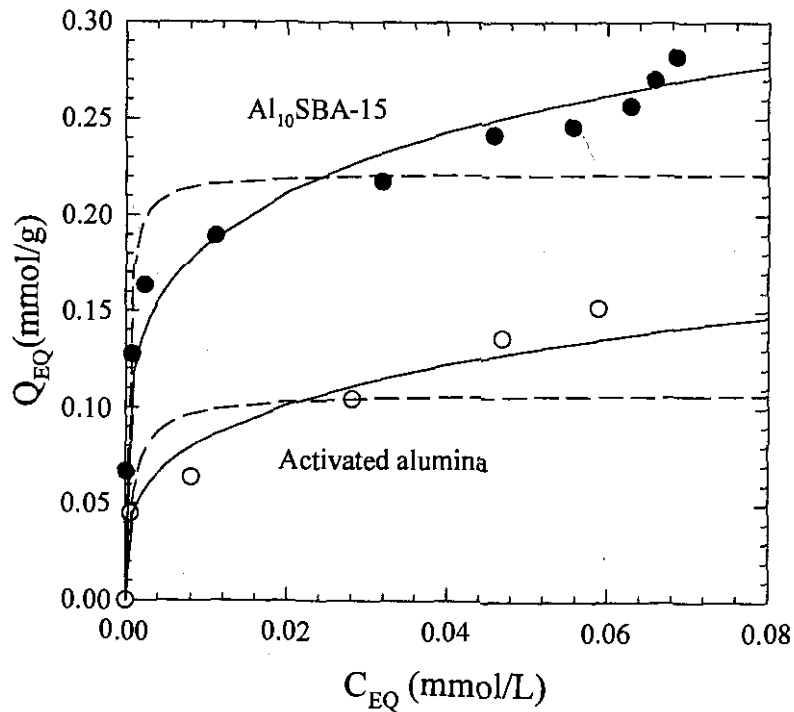
To determine the adsorption capacities of Al<sub>10</sub>SBA-15 and activated alumina for low initial arsenic concentration, adsorption isotherm tests were performed in a low arsenic concentration of 0.133 mmol/L or 10 mg/L. (Figure 4). The solution volume was 100 mL and masses of both adsorbents were varied. The filtrate was analyzed for arsenate concentration of solution with AAS-graphite methods. The final pH was fixed at 6.55 ± 0.02. From fitting data with the Freundlich isotherm, the arsenic adsorption capacity of Al<sub>10</sub>SBA-15 was determined to be 0.185 mmol/g, which is 2.2 times greater than that of activated alumina (0.084 mmol/g) at 0.1 mmol/L initial arsenic concentration. Based on the mole fraction of arsenate and each metal compound, the observed adsorption densities for activated alumina and Al<sub>10</sub>SBA-15 were 0.00857 mmol<sub>As</sub>/mmol<sub>Al</sub> and 0.05 mmol<sub>As</sub>/mmol<sub>Al</sub> at 0.1 mmol/L initial concentration, respectively. The fitting parameters and determination coefficient R<sup>2</sup> values for activated alumina and Al<sub>10</sub>SBA-15 are summarized in Table 3. This result is very similar to adsorption isotherm data that were obtained with a higher arsenic initial concentration.

Figure 5 shows the adsorption isotherm data of activated alumina and Al<sub>10</sub>SBA-15 under different pH conditions at an equilibrium state. Arsenate adsorption capacities of Al<sub>10</sub>SBA-15 were linearly increased with the decrease in pH, while activated alumina did not show significant changes in adsorption capacities. At pH 7.0, Al<sub>10</sub>SBA-15 had about 0.2 mmol As/g of adsorption capacity, which is twice as large as for activated alumina. Even though the adsorption capacities of Al<sub>10</sub>SBA-15 were much greater than other adsorption studies (Grossl *et al.*, 1997; Manning *et al.*, 1998), the adsorption tendency of Al<sub>10</sub>SBA-15 under different pH conditions at equilibrium was very similar to the other studies' equilibrium, in which oxyanion adsorption on goethite was investigated. This

result suggests that Al<sub>10</sub>SBA-15 had inner-sphere complexes for arsenate adsorption as in other studies. Inner-sphere complexes can be explained by the fact that oxyanions are bonded covalently with the reactive functional groups on the surface without a hydration reaction.

**Table 3. Determination Coefficients (R<sup>2</sup>) and Parameters for the Fit of Arsenate Adsorption Isotherm Data to Both *Freundlich* and *Langmuir* Isotherms**

Adsorption isotherms and parameters		Activated alumina	Al <sub>10</sub> SBA-15
Langmuir	b	1049.88	3518.82
	Q <sub>max</sub> (mmol/g)	0.120	0.283
	R <sup>2</sup>	0.765	0.933
Freundlich	K	0.291	0.455
	n	0.269	0.196
	R <sup>2</sup>	0.924	0.960



**Figure 4 - Arsenate adsorption isotherm (pH = 6.55, shaker temperature = 25 ± 0.5°C, the ionic strength made by NaNO<sub>3</sub> = 0.01 M).**

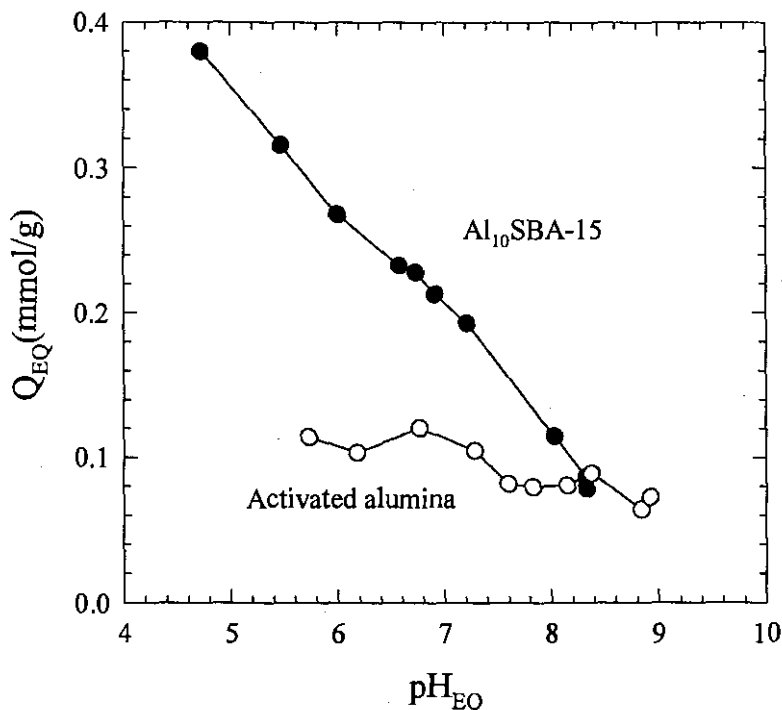


**Figure 5 - Adsorption isotherm data of activated alumina and Al<sub>10</sub>SBA-15 under different pH conditions at equilibrium state.**

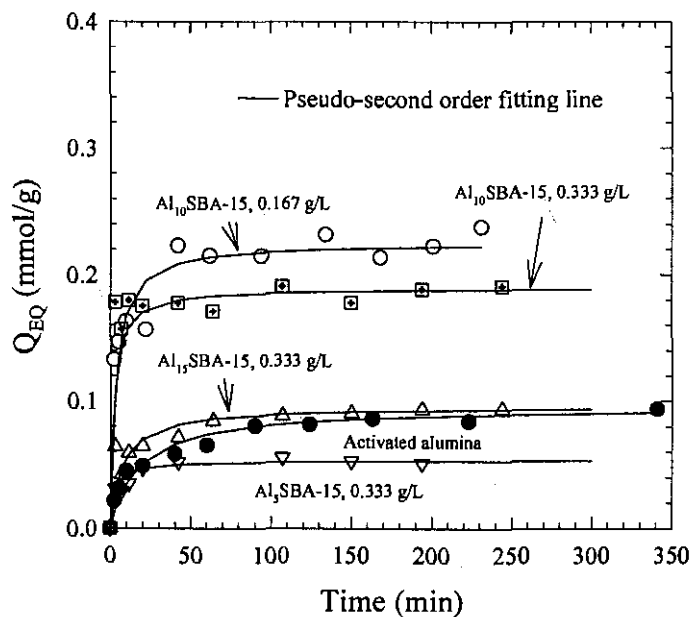
#### **Kinetic studies of arsenic adsorption**

Figure 6 shows the arsenate adsorption kinetic data of activated alumina, Al<sub>5</sub>SBA-15, Al<sub>10</sub>SBA-15, and Al<sub>15</sub>SBA-15 as well as their fitting lines of the pseudo second order kinetic model, which had the highest determination coefficient ( $R^2$ ) values for all data (Table 4). The determination coefficients ( $R^2$ ) and parameter values of  $q_{eq}$  ( $\text{mmol}_{As}/\text{mmol}_{Al}$ ) and initial sorption rate ( $v_0$ ) for different kinetic models are summarized in Table 4. Figure 7 shows the overall diffusion adsorption rate constants obtained from the parabolic diffusion kinetic model and  $q_{eq}$  ( $\text{mmol}_{As}/\text{g}$ ) values obtained from the pseudo second order kinetic model.

Compared with activated alumina, Al<sub>10</sub>SBA-15 had a very fast arsenic adsorption rate, in which equilibrium was reached within 1 hr. In addition, the adsorption capacity of Al<sub>10</sub>SBA-15 was twice as great as that of activated alumina. Al<sub>10</sub>SBA-15 showed the highest adsorption rate and capacity for different solid concentrations even if arsenic adsorption capacities for all aluminum impregnated SBA-15 solids decreased with higher solid concentration, which had the same phenomena as the adsorption isotherm data fitted with the Freundlich isotherm model. Al<sub>2.5</sub>SBA-15 and Al<sub>5</sub>SBA-15 had lower adsorption capacity (in  $\text{mmol}_{As}/\text{g}$ ) than activated alumina. Al<sub>15</sub>SBA-15 had slightly higher adsorption capacity than activated alumina but much lower than Al<sub>10</sub>SBA-15 at 0.333 g/L solid concentration. The initial sorption rate and  $k_{diff}$  of Al<sub>15</sub>SBA-15 were 0.0128 ( $\text{mmol g}^{-1} \text{min}^{-1}$ ) and 0.457 ( $\text{min}^{-0.5}$ ), respectively. The initial sorption rate of Al<sup>10</sup>SBA-

15 ( $0.0824 \text{ mmol g}^{-1} \text{ min}^{-1}$ ) was 15 times greater than that of activated alumina ( $0.0054 \text{ mmol g}^{-1} \text{ min}^{-1}$ ) at  $0.333 \text{ g/L}$  solid concentration. These results show great advantages of  $\text{Al}_{10}\text{SBA-15}$  for POE/POU application due to its rapid and high adsorption capacity.

Among five different kinetic models, two kinetic models such as the pseudo second order and parabolic diffusion kinetic models had very high determination coefficients ( $R^2$ ). The pseudo second order kinetic model is usually related to the adsorption process that has the exchange reaction as the rate-controlling step (Aretxaga *et al.*, 2001). Therefore, it was found that the exchange reaction in which arsenate adsorption for adsorbents resulted in  $\text{OH}^-/\text{H}^+$  release was the rate-controlling step for these kinetic studies. This result was verified by (Jain *et al.*, 1999), in which they tried to solve the  $\text{H}^+/\text{OH}^-$  release mechanisms with arsenic adsorption onto ferrihydrite. The diffusion of adsorbate was also the rate-controlling step of arsenic adsorption due to high determination coefficients for the parabolic diffusion kinetic model. This result was similar to other studies (Raven *et al.*, 1998; Li, 1999). However, the  $R^2$  values of the simple Elovich model were relatively low for all data of aluminum incorporated SBA-15, which suggested that the adsorption reaction of arsenate is not slow for active sites of adsorbents.



**Figure 6 - Kinetics of arsenate adsorption at  $\text{pH } 7.2 \pm 0.02$  with  $0.133 \text{ mmol/L}$  arsenic initial concentrations.**

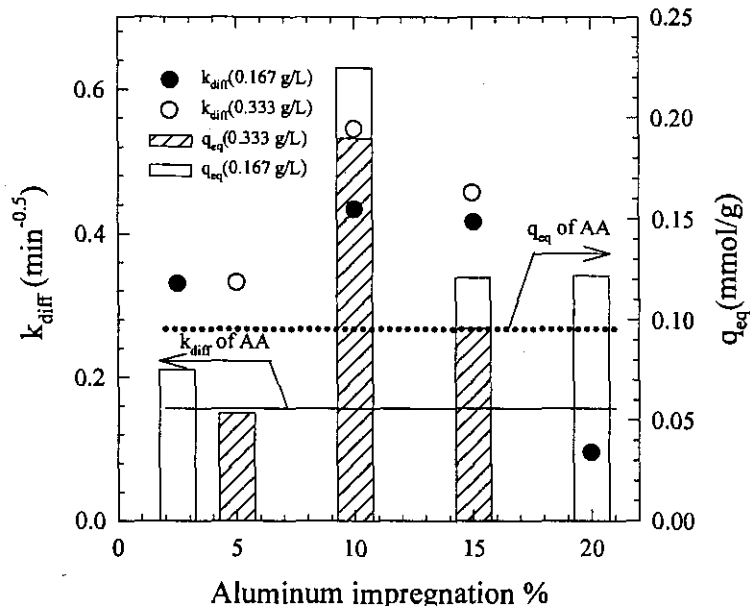


Figure 7 –Overall diffusion adsorption rate constants and  $q_{eq}$  values for all kinetic data.

Table 4 - Determination Coefficients ( $R^2$ ) of Different Kinetic Model Fitting of Arsenic Adsorption Kinetics for Activated Alumina and AISBA-15.

Adsorbents	Kinetic Models Solid conc. (g/L)	Pseudo First Order	Pseudo Second order	Power Function	Simple Elovich	Parabolic Diffusion	Parameters	
		Determination Coefficients ( $R^2$ )						$^1v_0$
AA	0.333	0.951	0.995	0.955	0.981	0.995	0.0054	0.0049
2.5%	0.167	0.487	0.937	0.465	0.418	0.982	0.0051	0.0812
5%	0.333	0.718	0.997	0.516	0.491	0.948	0.0189	0.0289
10%	0.167	0.688	0.997	0.871	0.856	0.962	0.0661	0.0607
	0.333	0.481	0.998	0.367	0.376	0.927	0.0824	0.0513
15%	0.167	0.701	0.984	0.654	0.601	0.972	0.0325	0.0218
	0.333	0.903	0.999	0.721	0.790	0.878	0.0128	0.0172
20%	0.167	0.822	0.963	0.847	0.846	0.923	0.0043	0.0165

$^1v_0$  ( $\text{mmol g}^{-1} \text{min}^{-1}$ ) and  $^2q_{eq}$  ( $\text{mmol}_{As}/\text{mmol}_{Al}$ ) were obtained by Pseudo Second Order kinetic model.

## SUMMARY AND CONCLUSIONS

From x-ray diffraction, it was found that aluminum 10% impregnation was safely incorporated by an incipient wetness impregnation technique for SBA-15, which had 638.75 m<sup>2</sup>/g of BET surface area and 48 Å of D<sub>BH</sub> (pore diameter), without producing clogging of pore structures. All adsorption isotherm and kinetic data of aluminum incorporated SBA-15 were compared with activated alumina, which has been widely used for adsorption processes of the POE/POU system. Al<sub>10</sub>SBA-15 showed about 2.2 ~ 2.4 times higher arsenate adsorption capacities than activated alumina in a broad range of arsenate initial concentration. The *Freundlich* isotherm model fit very well with all isotherm data that were performed under different arsenate initial concentrations. Arsenate adsorption capacities of Al<sub>10</sub>SBA-15 increased linearly with the decrease in pH, while activated alumina did not show significant changes in adsorption capacities. Although the adsorption capacities of Al<sub>10</sub>SBA-15 were much higher, the result was very similar to other studies which suggested that oxyanions follow the inner-sphere complexes models.

Among five different kinetic models, two kinetic models, namely the pseudo second order and parabolic diffusion kinetic models, had very high determination coefficients (R<sup>2</sup>) for all kinetic data. Therefore, it appeared that the rate-controlling step of arsenate adsorption for all adsorbents can be explained by both an exchange reaction and a diffusion reaction. Al<sub>10</sub>SBA-15 showed the maximum adsorption rates and capacities under different solid concentrations, in which the initial sorption rate and q<sub>eq</sub> values of Al<sub>10</sub>SBA-15 were more than 15 and 2 times greater than those of activated alumina at a 0.333 g/L solid concentration, respectively. These results show great advantages of Al<sub>10</sub>SBA-15 for POE/POU application due to its rapid and high adsorption capability.

## ACKNOWLEDGMENT

This research was supported by grants from the Industrial and Economic Development Research Fund (I&EDR) for University-Industry Relations of the University of Wisconsin-Madison, the Applied Research Grant of the University of Wisconsin System, and the Groundwater Research Council of the Department of Natural Resources (DNR), Wisconsin.

## REFERENCES

- Aretxaga, A.;Romero, S.;Sad, M.; and Vicent, T. (2001). Adsorption Step in the Biological Degradation of a Textile Dye. *Biotechnol. Prog.*, 664.
- Chris, L. X.;Yalcin, S.; and Mingsheng, M. (2000). Speciation of Submicrogram per Liter Levels of Arsenic in Water: On-Site Species Separation Integrated with Sample Collection. *Environ. Sei. Technol.*, **34**, 2342.
- Chwirka, J. D.;Thomson, B. M.; and Stomp III, J. M. (2000). Removing arsenic from groundwater. *AWWA*, **92**, 79.
- Gilles, G. C. (2000). Advancing Arsenic Adsorption, Specialty media can be used for POU/POE systems. *Water Technology*, **September** 2000.

- Grossl, P. R.;Eick, M.;Sparks, D. L.;Goldberg, S.; and Ainsworth, C. C. (1997). Arsenate and Chromate Retention Mechanisms on Goethite. 2. Kinetic Evaluation Using a Pressure-Jump Relaxation Technique. *Environ. Sci. Technol.*, **31**, 321.
- Jain, A.;Raven, K. P.; and Loeppert, R. H. (1999). Arsenite and Arsenate Adsorption on Ferrihydrite: Surface Charge Reduction and Net OH<sup>-</sup> Release Stoichiometry. *Environ. Sci. Technol.*, **33**, 1179.
- Johnston, R.; and Heijnen, H. (2001). Safe Water Technology for Arsenic Removal. Dhaka, Bangladesh University of Engineering and Technology.
- Kresge, C. T.;Leonowicz, M. E.;Roth, W. J.;Vartuli, J. C.; and Beck, J. S. (1992). Ordered Mesoporous Molecular Sieves by a Liquid-crystal Template Mechanism. *Nature*, **359**, 710.
- Kruk, M.;Jaroniec, M.;Ko, C. H.; and Ryoo, R. (2000). Characterization of the Porous Structure of SBA-15. *Chem. Mater.*, **12**, 1961.
- Li, Z. (1999). Sorption Kinetics of Hexadecyltrimethylammonium on Natural Clinoptilolite. *Langmuir*, **15**, 6438.
- Manning, B. A.;Fendorf, S. E.; and Goldberg, S. (1998). Surface Structures and Stability of Arsenic(III) on Goethite: Spectroscopic Evidence for Inner-Sphere Complexes. *Environ. Sci. Technol.*, **32**, 2383.
- Margolese, D.;Melero, J. A.;Christiansen, S. C.;Chmelka, B. F.; and Stucky, G. D. (2000). Direct Syntheses of Ordered SBA-15 Mesoporous Silica Containing Sulfonic Acid Groups. *Chem. Mater.*, **12**, 2448.
- Namasivayam, C.; and Senthilkumar, S. (1998). Removal of Arsenic(V) from Aqueous Solution Using Industrial Solid Waste: Adsorption Rates and Equilibrium Studies. *Ind. Eng. Chem. Res.*, **37**, 4816.
- Newalkar, B. L.;Olanrewaju, J.; and Komarneni, S. (2001). Direct Synthesis of Titanium-Substituted Mesoporous SBA-15 Molecular Sieve under Microwave-Hydrothermal Conditions. *Chem. Mater.*, **13**, 552.
- Raven, K. P.;Jain, A.; and Loeppert, R. H. (1998). Arsenite and Arsenate Adsorption on Ferrihydrite: Kinetics, Equilibrium, and Adsorption Envelopes. *Environ. Sci. Technol.*, **32**, 344.
- Sing, K. S. W.;Everett, D. H.;Haul, R. A. W.;Moscow, L.;Pierotti, R. A.;Rouquerol, J.; and Siemieniewska, T. (1985). Reporting Physisorption Data for Gas/solid Systems with Special Reference to the Determination of Surface Area and Porosity. *Pure Appl. Chem.*, **57**, 603.
- Viraraghavan, T.;Subramanian, K. S.; and Aruldoss, J. A. (1999). Arsenic in Drinking Water - Problems and Solutions. *Wat. Sci. Tech.*, **40**, 69.
- Woods, R. (2001). EPA Announces Arsenic Standard for Drinking Water of 10 Parts Per Billion. *Headquarters Press Release, Environmental News*.
- Zhao, D.;Feng, J.;Huo, Q.;Melosh, N.;Fredrickson, G. H.;Chmelka, B. F.; and Stucky, G. D. (1998). Triblock Copolymer Syntheses of Mesoporous Silica with Periodic 50 to 300 Angstrom Pores. *SCIENCE*, **279**, 548.
- Zhao, D.;Sun, J.;Li, Q.; and Stucky, G. D. (2000). Morphological Control of Highly Ordered Mesoporous Silica SBA-15. *Chem. Mater.*, **12**, 275.

Jang, Min; Shin, Eun Woo; Park, Jae Kwang. 2002 Removal of arsenic using mesoporous silicate media impregnated metal oxides nano-particles. In: Proceedings of WEFTEC 2002-the water quality event; 2002 October 2; Chicago IL. Alexandria, VA: Water Environment Federation. 15 p.